1

2

3

The genomic health of ancient hominins

5

6

7   Ali J. Berens[1], Taylor L. Cooper[1], and Joseph Lachance[1*]

8

9

10

11   [1]School of Biological Sciences, Georgia Institute of Technology, Atlanta, GA 30332

12   *lachance.joseph@gmail.com

13

14

15

16   Keywords: ancient DNA, genetic disease risks, human evolution, population genetics,

17   predictive health

18 **ABSTRACT**

19 The genomes of ancient humans, Neandertals, and Denisovans contain many alleles

20 that influence disease risks. Using genotypes at 3180 disease-associated loci, we

21 estimated the disease burden of 147 ancient genomes. After correcting for missing

22 data, genetic risk scores were generated for nine disease categories and the set of all

23 combined diseases. These genetic risk scores were used to examine the effects of

24 different types of subsistence, geography, and sample age on the number of risk alleles

25 in each ancient genome. On a broad scale, hereditary disease risks are similar for

26 ancient hominins and modern-day humans, and the GRS percentiles of ancient

27 individuals span the full range of what is observed in present day individuals. In

28 addition, there is evidence that ancient pastoralists may have had healthier genomes

29 than hunter-gatherers and agriculturalists. We also observed a temporal trend whereby

30 genomes from the recent past are more likely to be healthier than genomes from the

31 deep past. This calls into question the idea that modern lifestyles have caused genetic

32 load to increase over time. Focusing on individual genomes, we find that the overall

33 genomic health of the Altai Neandertal is worse than 97% of present day humans and

34 that Ötzi the Tyrolean Iceman had a genetic predisposition to gastrointestinal and

35 cardiovascular diseases. As demonstrated by this work, ancient genomes afford us new

36 opportunities to diagnose past human health, which has previously been limited by the

37 quality and completeness of remains.

2

INTRODUCTION

Ancient human remains yield valuable information about the health and disease of individuals from the past. Skeletal remains provide details about medical practices (Andrushko and Verano 2008) and certain diseases, such as cancers (Binder, et al. 2014; Odes, et al. 2016) and rheumatic diseases (Entezami, et al. 2011) that visibly alter or affect bone. However, many diseases do not leave their mark on bone; instead, they cause soft tissue damage requiring mummified remains for diagnosis. One of the best studied set of mummified human remains is the Tyrolean Iceman, a well-preserved 5300-year-old Neolithic man discovered in the Ötztal Alps. Examination of his remains shows hardening arteries suggesting that this man possessed a predisposition for coronary heart disease (Murphy, et al. 2003). Further evidence from the sequencing of the Iceman's genome supports this diagnosis (Keller, et al. 2012) and demonstrates that modern risk alleles can accurately predict disease risk in ancient individuals. In addition to heart disease, genetic data also indicate that the Iceman was likely lactose intolerant, had type O blood, and had brown eyes (Keller, et al. 2012). Unfortunately, not all ancient human samples are as complete and well-preserved as the Tyrolean Iceman. Genomic information may shed new light on the health of ancient individuals, especially when soft tissue and skeletal evidence are unavailable.

To estimate the health of different individuals, genetic information can be converted into a quantitative measure of hereditary disease burden, which we refer to as a genetic risk score (GRS). GRS have already been used to estimate disease risk in modern humans (Chatterjee, et al. 2016). Assuming that disease loci act independently, one way to calculate GRS is to sum the number of risk alleles across all disease loci

61   after weighting each allele by its effect size (Corona, et al. 2013). The majority of known

62   disease alleles have been identified in present-day Europeans through genome wide

63   association studies (GWAS) using microarrays, which are known to contain a biased set

64   of genetic variants (Lachance and Tishkoff 2013). Despite this bias, genetic risk scores

65   can still be informative about disease risk. For example, GRS for breast, colorectal, and

66   bladder cancer and coronary heart disease accurately predict risk of each disease while

67   offering insights into prevention and treatment options (Chatterjee, et al. 2016). Not only

68   can GRS be applied to specific traits, but genetic risk can also be estimated for the

69   entire genome.

70   One significant limitation of ancient DNA studies is that most genomes are not

71   complete, which makes it more challenging to estimate disease risk. Genomes may be

72   incomplete due to contamination (Orlando, et al. 2015), DNA degradation (Hofreiter, et

73   al. 2015), or low coverage sequencing, as has been the case with large cohort studies

74   (Mathieson, et al. 2015; Lazaridis, et al. 2016). One approach to address missing

75   genomic data is to impute genotypes at disease-associated loci (Sainz, et al. 1989; Li,

76   Willer, et al. 2009). However, imputation of ancient genotypes is challenging because of

77   small sample sizes. To avoid imputation errors, genetic risk scores for each ancient

78   sample can be calculated using only loci with successful genotype calls (i.e. genetic risk

79   scores for each sample use a different set of disease loci). Each ancient genome can

80   then be compared to modern genomes at a matched set of disease loci to generate

81   standardized GRS percentiles, which enables comparisons between different ancient

82   genomes.

83   There has been recent debate about whether rates of sequence change in

84   human genomes have increased over time. Hawks, et al. (2007) suggest that rates of

85   adaptive evolution have been accelerating over the last 40,000 years, especially within

86   the last 5,000 years. The holocene has brought new selective pressures associated with

87   the transition from hunting and gathering to agricultural practices (Hawks, et al. 2007).

88   Genes involved in subsistence and dietary changes along with disease resistance

89   genes show strong positive selection (Hawks, et al. 2007; Field, et al. 2016). Others

90   have argued that there has not been enough time for selection to expel deleterious

91   alleles that lead to evolutionary mismatches between our genomes and modern

92   environments (Cordain, et al. 2005). More recently, modern medicine and changes in

93   living conditions may have led to the relaxation of selective pressures within the last

94   century. Along these lines, Lynch (2016) argues that there has been a substantial

95   increase in the mutational load of modern humans (on the order of 1% reduction in

96   fitness per generation). However, Roth and Wakeley (2016) contend that the relaxation

97   of selective pressures is not as severe as suggested by Lynch (2016).

98   With this debate in mind, our study estimated the genomic health of ancient

99   individuals by combining disease-association information from the NHGRI-EBI GWAS

100   Catalog with publicly available genomes of ancient hominin samples. We investigated

101   relationships between genetic disease risk and sample age. We further explored this

102   dataset by determining whether genetic risks vary for individuals who practiced different

103   types of subsistence and examined whether ancient GRS follow a geographic cline.

104   Finally, we probed differences in genomic health between modern and ancient hominins

105   by calculating genetic risk scores for different disease categories.

106

107

MATERIALS AND METHODS

Disease-associated loci

The set of all known autosomal disease-associated alleles was downloaded from

the NHGRI-EBI Catalog of published GWAS studies (www.ebi.ac.uk/gwas; last

accessed on September 28, 2016) (Burdett, et al. 2016; MacArthur, et al. 2017). Any

non-disease-associated alleles (e.g., hair color, blood pressure, and amount of sleep)

were removed from consideration. We also filtered out disease-associated alleles from

the GWAS Catalog that were missing p-value, odds ratio, and/or allele frequency

information. When SNPs were associated with the same disease in multiple GWAS, we

retained the SNP with the strongest disease association (i.e. lowest p-value). To ensure

independence between variants associated with a given disease, we included only loci

that were not in linkage disequilibrium with other disease variants. This involved keeping

the strongest disease association (i.e. lowest p-value) whenever two SNPs were located

within 100kb of each other. After filtering, we were left with 3180 autosomal disease-

associated alleles from 578 GWAS. We classified all remaining disease-associated loci

into nine categories (allergy/autoimmune, cancers, cardiovascular, dental/periodontal,

gastrointestinal/liver, metabolism/weight, miscellaneous, morphological/muscular, and

neurological/psychological). These disease categories are not mutually exclusive, so a

single locus could be grouped into multiple categories (e.g., Crohn's disease is both an

autoimmune and a gastrointestinal disease). Note that many disease-associated loci

tend are older SNPs that have intermediate frequency alleles (Lachance 2010).

6

129   Because of this, many GWAS alleles can also be found in Neanderthal and Denisovan

130   genomes.

131

Ancient hominin genomes

133   We downloaded all known publicly available ancient hominin genomes (449

134   genomes as of July 1, 2016) and identified genotypes at the 3180 focal disease-

135   associated loci. For genomes that were only available as alignments to the human

136   reference genome, we called genotypes from these alignments using the 'mpileup'

137   function in SAMtools (v. 1.3) (Li, Handsaker, et al. 2009; Li 2011). We retained ancient

138   hominin samples that had genotype calls at greater than fifty percent of the focal 3180

139   disease-associated loci, after which 147 ancient genomes from 22 studies remained.

140   This filter was used to ensure sufficient genotype information for subsequent analyses.

141   Figure 1 displays the geographic locations of the 147 focal ancient individuals, which

142   were jittered to clarify densely sampled locations.

143

Modern human genomes

145   We downloaded modern human genomes from phase 3 of the 1000 Genomes

146   Project (The 1000 Genomes Project Consortium 2015), and we integrated this genomic

147   data with our 3180 focal disease-associated loci. At each of the 3180 loci, we obtained

148   the allele frequencies for the five continental super-populations of modern humans from

149   the 1000 Genomes Project (AFR, AMR, EAS, EUR, and SAS).

150

Genetic risk scores

7

152   For each ancient sample, we estimated GRS across all diseases and for each

153   disease category by combining genotypic information and effect sizes. All ancient

154   hominins were missing genotypic information at some of the disease-associated loci. To

155   account for this missing information, we calculated GRS for each ancient individual (i)

156   from the set of disease-associated loci with genotypic calls in that individual (L_i):

157    $$GRS_i = \sum_{l=1}^{L_i} \beta_l \times (\text{\# of copies of the risk allele at locus } l \text{ in ancient individual } i$$

158   where $\beta_l = ln$ (odds ratio at locus l). Because each ancient sample contains a different

159   set of disease-associated loci with genotype calls, GRS are not directly comparable

160   across individuals.

161   To enable comparisons across individuals, we converted raw GRS statistics into

162   standardized GRS percentiles (see Figure 2 for a pictorial representation). For each

163   ancient genome, this involved simulating 100,000 modern individuals at a matched set

164   of disease loci. Genotypes at disease loci were simulated for 20,000 modern individuals

165   for each of the five super-population from the 1000 Genomes Project (AFR, AMR, EAS,

166   EUR, and SAS). Each diploid genotype was drawn from a binomial distribution using the

167   'rbinom' function in R where the probability of drawing each risk allele is equal to the

168   allele frequency for the given super-population. These simulations assume that disease

169   loci are independent (i.e. they are in linkage equilibrium). Sites that were uncalled in the

170   focal ancient genome were masked in the simulations of modern genomes. Genetic risk

171   scores were then calculated for each modern individual (j) using a matched set of called

172   loci (L_i) for each focal ancient individual (i):

8

173 $$GRS_{i,j} = \sum_{l=1}^{L_i} \beta_l \times (\text{\# of copies of the risk allele at locus } l \text{ in modern individual } j)$$

174   Then, we compared the genetic risk score of each ancient individual to the distribution

175   of the simulated modern genetic risk scores using the empirical cumulative density

176   function (ecdf) function in R. This enabled us to obtain the percentile rank of each

177   ancient sample relative to modern individuals, i.e. the standardized GRS percentile of

178   each ancient genome. We repeated this standardization process for each ancient

179   genome, then used the standardized GRS percentiles to compare genetic risk amongst

180   ancient individuals and between ancient and modern hominins. Higher percentiles

181   indicate less healthy genomes. Standardized GRS percentiles were calculated for the

182   set of all combined diseases and for each disease category. Ancient genomes with risk

183   scores below the range of their matched set of modern genomes have standardized

184   GRS percentiles of 0%, and ancient genomes with risk scores above the range of their

185   matched set of modern genomes have standardized GRS percentiles of 100%. An R

186   Shiny (Chang, et al. 2017) interactive web application of our results can be found at:

187   http://popgen.gatech.edu/ancient-health/.

188

189   **Statistical tests**

190   For the set of all disease-associated SNPs and each disease category, we tested

191   for differences between the GRS of modern humans and ancient hominins. By

192   definition, the GRS percentiles of modern humans follow a uniform distribution that

193   ranges between zero and one. If ancient hominins have the same genomic risk of

194   disease as modern humans, the standardized GRS percentile of ancient samples will

9

195   also be uniformly distributed. We used a Kolmogorov-Smirnov test to determine whether

196   the distribution of ancient hominin standardized GRS percentiles is, in fact, uniformly

197   distributed. With Wilcoxon signed rank tests and continuity corrections, we also tested

198   for a shift in the ancient hominin standardized GRS percentile distribution compared to

199   the expectation of the modern human distribution (centered around 0.5).

200   Amongst the ancient hominin samples, we investigated whether there are

201   relationships between standardized GRS percentile and sample age, mode of

202   subsistence, and geographic location. These tests were run for all disease loci (overall

203   GRS percentiles) and by disease category. We separated ancient samples into six

204   sample age bins (n = number of samples; < 3500 [n = 20], 3500-4999 [n = 48], 5000-

205   6499 [n = 34], 6500-7999 [n = 10], 8000-9499 [n = 24], and ≥ 9500 years before present

206   [n = 11]). We then tested whether there is a difference in standardized GRS percentile

207   based on sample age bin using a Kruskal-Wallis test. The Kruskal-Wallis test is a rank-

208   based nonparametric test that can be used to determine if the differences between two

209   or more groups are significant. Following rejection of this test, we performed post-hoc

210   multiple pairwise comparisons using Dunn tests to determine which ages were

211   significantly different from each other. Dunn tests generate z-statistics from rank sums.

212   The Benjamini-Hochberg method was used to correct for multiple comparisons. We also

213   used a Jonckheere-Terpstra test, similar to Kruskal-Wallis except that the alternative

214   hypothesis is ordered, to determine whether standardized GRS percentile increased

215   with sample age bin. Mode of subsistence varies across ancient samples (n = number

216   of samples; agriculturalist [n = 106], hunter-gatherer [n = 22], and pastoralist [n = 19]).

217   Differences in standardized GRS percentiles due to mode of subsistence were

10

218   assessed by Kruskal Wallis tests followed by post-hoc pairwise multiple comparisons

219   with Dunn tests. These non-parametric tests do not require groups to have equal

220   sample sizes. Using Pearson's correlation, we also tested for an association between

221   standardized GRS percentile and North-South (latitude) or East-West (longitude)

222   gradients.

223

224   **RESULTS**

225   **Overall genetic risks**

226   On the whole, ancient samples had GRS that were similar to individuals living in

227   the present (Figure 3A; Supplemental Table S1). Figure 3A shows that the distribution

228   of standardized GRS percentiles of ancient individuals spans the full range of modern

229   humans. In general, most GRS scores are evenly distributed. However, there is an

230   excess of ancient hominins who have standardized GRS percentiles below 5%, which

231   causes the distribution of standardized GRS percentiles to be positively skewed

232   (Kolmogorov-Smirnov test, D = 0.265, p-value = 2.04×10^{-9}). Using a Wilcoxon signed

233   rank test, we find that the ancient samples have, on average, lower predicted genomic

234   risk than modern humans (Table 1). However, GRS calculations for ancient samples

235   may underestimate the total amount of genetic risk, as many disease alleles that

236   segregated in the past remain undiscovered.

237   Data quality of the ancient genomes varies across samples, so we also tested

238   whether there were any systematic biases in GRS calculations due to sample quality.

239   Both sequencing coverage and the proportion of disease loci that are called may

240   potentially affect whether an individual has a high or low GRS. Based on Pearson's

11

241   correlation, there is a weak, yet significant, positive relationship between standardized

242   GRS percentiles and sequencing coverage for ancient samples (Figure 4A, R^2 = 0.087,

243   p-value = 3.0×10^{-4}). However, this pattern may be driven by a small number of outliers,

244   including the Altai Neandertal genome (sequencing coverage: 52x, standardized GRS

245   percentile: 97%). Encouragingly, standardized GRS percentiles are largely independent

246   of the proportion of disease-associated loci that are able to be successfully called in

247   each ancient sample (Figure 4B, R^2 = 0.013, p-value = 0.17). Taken together, these

248   patterns indicate that our GRS calculations are largely free of biases due to sample

249   quality.

250

251   *Effects of sample age*

252   Figure 3A clearly shows that disease risk varies greatly amongst ancient

253   hominins, so we investigated whether genetic risk scores follow a temporal pattern.

254   Samples were binned into six age ranges, the most recent of which includes individuals

255   that lived less than 3500 years before present and the oldest of which includes

256   individuals who lived at least 9500 years before present (BP). Among ancient samples,

257   there is a difference in the standardized GRS percentile based on sample ages

258   (Kruskal-Wallis test, χ^2 = 15.24, df = 5, p-value = 0.009). From Figure 3B, it is evident

259   that the oldest samples are at much greater genetic risk than more recent samples. We

260   compared standardized GRS percentiles between pairs of sample age ranges using

261   Dunn tests with Benjamini-Hochberg corrections and found that the oldest age range (≥

262   9500 years BP) is significantly higher than the two most recent age ranges (< 3500 and

263   3500-4999 years BP, p-values < 0.007). Following up on this result, we examined

12

264   whether genetic risks progressively improved with time. Results of a Jonckheere-

265   Terpstra test appear to support this proposition (p-value = 0.001; Table 1), as genetic

266   disease risk increased with later age ranges. This temporal trend is not due to

267   differences in sequence coverage. Our results are robust to the inclusion or exclusion of

268   archaic hominins: when Neanderthal and Denisovan samples are removed, the oldest

269   age class has a median GRS percentile of 0.88.

270

271   *Subsistence type*

272   The number of risk alleles in each ancient genome may also vary by the mode of

273   subsistence, i.e. whether individuals practiced a hunter-gatherer, agricultural, or

274   pastoral lifestyle. We tested this hypothesis by performing a Kruskal-Wallis test.

275   Comparisons of ancient standardized GRS indicate that form of subsistence affects

276   estimated genetic risk of disease (Table 1). Following up on this result, we used a post-

277   hoc Dunn test with Benjamini-Hochberg correction to determine which types of

278   subsistence are different from each one another. Pastoralists have significantly lower

279   standardized GRS percentiles than agriculturalists and hunter-gatherers, while the

280   standardized GRS percentiles are not significantly different between agriculturalists and

281   hunter-gatherers (Table 2). Figure 3C shows that the distribution of standardized GRS

282   percentiles for ancient pastoralists is shifted into to the healthy range of modern

283   humans. We find that the genomes of ancient pastoralists have standardized GRS

284   percentiles almost exclusively below the 50th percentile of modern humans. In contrast,

285   predictions of disease risk in the genomes of ancient agriculturalists and hunter-

286   gatherers span the full range of modern humans.

13

287   One possible concern is that sequencing coverage and the proportion of disease-

288   associated loci that were successfully called vary by subsistence type (Kruskal-Wallis

289   tests, p-values = 0.03 and 0.01, Figure 4E and 4F, respectively). Differences in

290   sequencing coverage between pastoralists and hunter-gatherers appear to be driven by

291   three older hominin samples – Altai Neandertal (52x), Ust'-Ishim (42x), and Denisovan

292   (30x). However, these differences in sequencing coverage do not lead to significant

293   differences in the proportion of disease-associated loci that are called in the genomes of

294   pastoralists and hunter-gatherers.

295

296   *Geographic patterns*

297   We tested whether genetic estimates of disease risks vary geographically (Table

298   1). Comparing standardized GRS percentiles and latitude, we find that northern ancient

299   individuals tend to have healthier genomes (Pearson correlation test, r = -0.23, p-value

300   = 5.0×10^{-3}). Interpretation of these results should be tempered by two considerations:

301   1) most of the ancient samples with sequence data were discovered in Eurasia and 2)

302   there is substantial heterogeneity in genetic risk scores across space. In contrast to

303   latitudinal patterns, the relationship between standardized GRS percentile and longitude

304   does not reach statistical significance (r = -0.13, p-value = 0.11). Despite heterogeneity

305   in standardized GRS percentiles and limited sampling, our results suggest that genetic

306   disease risks may have followed a North-South geographic cline in the past.

307

308   **Disease Categories**

14

309 Which types of diseases drive differences in genetic risk scores between ancient

310 and modern individuals? To address this question, we also estimated genetic risk of

311 ancient hominins for nine disease categories (Supplemental Table S1). On average,

312 ancient individuals had significantly lower genetic risk of cancers, miscellaneous

313 diseases, and neurological/psychological diseases than modern humans (Figure 5A; p-

314 values < 0.05). Table 1 lists summary statistics and p-values from Wilcoxon signed

315 ranked tests for each disease category. Only cardiovascular-associated diseases were

316 predicted to have greater risk in ancient hominins compared to modern humans (p-

317 value = 1.8×10^{-5}). Risks of allergy/autoimmune, morphological/muscular,

318 metabolism/weight, and dental/periodontal diseases were not significantly different

319 between ancient and modern hominins (p-values > 0.05). Thus, the genetic disease

320 burden of ancient hominins appears to be less than modern humans due to reduced risk

321 of cancer and neurological disease along with other unclassified diseases.

322

323 *Effects of sample age with respect to disease categories*

324 We calculated genetic risks for nine disease categories to determine whether

325 temporal trends were consistent across each disease type. Figure 5B displays the

326 standardized GRS percentile by disease category summarized for each sample age

327 range. Broadly speaking, we find that genetic disease risks change over time. Some

328 disease categories show progressive changes over time. Using Jonckheere-Terpstra

329 tests, we find that older samples have higher standardized GRS percentiles for

330 allergy/autoimmune diseases, cancers, and gastrointestinal/liver diseases (p-values <

331 0.05). Temporal trends for metabolic diseases were marginally significant (p-value =

332   0.054). See Table 1 for complete results of Jonckheere-Terpstra tests by disease

333   category. Taken together, the time-dependent results suggest that more recent ancient

334   hominins have lower disease load due to reduced risk of immune-related and

335   gastrointestinal diseases, cancer, and metabolism-related disorders.

336

337   *Subsistence type and disease categories*

338   We tested whether differences in genetic risk for ancient individuals with different

339   modes of subsistence were consistent across all disease categories or whether a single

340   disease category drove disparities in genetic risk between subsistence groups. Using

341   Kruskal-Wallis tests, we find that form of subsistence affects predicted genetic risk of

342   allergy/autoimmune diseases, cancers, dental/periodontal diseases, and

343   gastrointestinal/liver diseases in ancient individuals (Figure 5C). Table 1 includes full

344   results from the Kruskal-Wallis test for each disease category. For each significant

345   disease category, we also performed post-hoc Dunn tests with Benjamini-Hochberg

346   correction; the z-statistics and p-values from these tests are displayed in Table 2. Both

347   the allergy/autoimmune and gastrointestinal/liver disease categories (which share many

348   of the same disease-associated loci) show significantly lower genetic risk in pastoralists

349   than agriculturalists and hunter gatherers. Pastoralists also have significantly reduced

350   risk for cancer compared to agriculturalists. Agriculturalists have a higher genetic risk for

351   dental/periodontal diseases than hunter-gatherers and pastoralists. In general,

352   pastoralists possess extremely healthy genomes, especially for cancers and immune-

353   related, periodontal, and gastrointestinal diseases.

354

16

355   *Geographic patterns and disease categories*

356   Finally, we examined geographic patterns in genetic risk scores for each disease

357   category using Pearson correlation tests (see Table 1 for results). For most disease

358   types, estimates of genetic risk did not follow a geographic cline. However, decreased

359   risk of disease in northern ancient individuals appears to be driven by two disease

360   categories: cancer (r = -0.29) and dental/periodontal diseases (r = -0.20). This negative

361   correlation between latitude and standardized GRS percentile is even stronger amongst

362   Eurasian ancient samples (cancer: r = -0.33; dental / periodontal diseases: r = -0.22).

363   Focusing on longitude, we estimate that the genetic risk of cardiovascular diseases was

364   lower for ancient individuals in the east compared to the west (r = -0.20). This trend is

365   slightly weaker when comparing only individuals from Eurasia (r = -0.18).

366

367   **Ancient precision medicine**

368   Although there are overarching patterns of risk based on type of subsistence and

369   sample age, each ancient individual has their own unique disease profile. These ancient

370   disease risk profiles are summarized in Table S1 and can be viewed via an interactive

371   web application: http://popgen.gatech.edu/ancient-health/. We found that the Altai

372   Neandertal had poor genomic health, with a standardized GRS of 97%. This was due in

373   part to high risk for immune-related diseases, cancers, gastrointestinal and liver

374   diseases, metabolic-related disorders, and morphological and muscular diseases.

375   However, the Altai Neandertal genome did not have an elevated number of risk alleles

376   for all disease classes – we estimated a low risk for cardiovascular disease and close to

377   average risk for periodontal and miscellaneous diseases. Our estimation of genetic risk

17

378   of cardiovascular disease for the Tyrolean Iceman supports previous evidence that this

379   ancient man had a predisposition for this disease (Keller, et al. 2012). Additionally, the

380   Tyrolean Iceman had high risk for immune-related diseases, gastrointestinal diseases,

381   and metabolic-related disorders. Despite these elevated risks, we also inferred that the

382   genome of the Iceman was relatively healthy for morphological and neurological

383   diseases.

384

385   **DISCUSSION**

386   Integrating ancient DNA with knowledge of disease associated loci from modern

387   populations provides new insights into past human health. Overall, we find that the GRS

388   percentiles of ancient hominins span the full range of modern humans. There are some

389   ancient individuals whose genomes place them among the healthiest or least healthy

390   individuals living in the present. Ancient individuals are enriched for standardized GRS

391   percentiles that are below 5% (Figure 3A), which may partially be explained by the fact

392   that our set of known disease-associated loci only includes genetic variants that

393   segregate in modern populations. Thus, we are excluding disease variants that

394   segregated in the past and possibly underestimating the GRS percentile of ancient

395   individuals, i.e. predicted scores are lower than the true genetic disease risk.

396   The genomic health of ancient individuals appears to have improved over time

397   (Figure 3B). This calls into question the idea that genetic load has been increasing in

398   human populations (Lynch 2016). However, there exists a perplexing pattern: ancient

399   individuals who lived within the last few thousand years have healthier genomes, on

400   average, than present day humans. This deviation from the observed temporal trend of

401   improved genomic health opens up the possibility that deleterious mutations have

18

402   accumulated in human genomes in the recent past. The data presented here do not

403   provide adequate information to address this hypothesis, which we leave for future

404   follow-up studies.

405   Genomic studies have shown that there are lingering effects of ancient

406   introgression on the health of modern-day humans. Here, we estimated that the Altai

407   Neandertal genome has an elevated risk of neurological diseases (80th percentile

408   compared to modern humans). This is consistent with previous findings from electronic

409   health records and patient genomes that linked Neandertal haplotypes with increased

410   risk for depression along with tobacco addiction, urinary tract disorders, and skin lesions

411   (Simonti, et al. 2016). Other studies have shown that Neandertal and Denisovan

412   introgression impacted the immune system of present-day humans (Abi-Rached, et al.

413   2011; Dannemann, et al. 2016; Deschamps, et al. 2016). In our study, the estimated

414   risk of immune-related diseases in Neandertal and Denisovan genomes were at the top

415   of the distribution (above 100% and 97% of all modern genomes, respectively). A

416   previous study showed that archaic alleles at three toll-like receptor genes are

417   associated with reduced microbial resistance and increased risk of allergic diseases

418   (Dannemann, et al. 2016). Despite these ill effects in modern environments, some

419   archaic alleles are quite prevalent in modern Europeans and Asians likely due to natural

420   selection (Deschamps, et al. 2016). For example, there is evidence that significant

421   changes to the coding regions of immunity related genes coincided with the shift in

422   subsistence from hunting and gathering to farming (Deschamps, et al. 2016). Our

423   results suggest that hunter-gatherers had higher genetic risk of allergy and autoimmune

424   disease compared to ancient agriculturalists and pastoralists.

19

425   There have been two great dietary shifts in recent human evolution: 1) the

426   consumption of carbohydrate rich diets with the onset of farming (approximately 10,000

427   years before present) and 2) the utilization of processed flour and sugar since the

428   industrial revolution (approximately 1850 AD). Compared to the other ancient hominins

429   with different forms of subsistence, we estimated that ancient pastoralists had healthier

430   genomes due to low risk for immune-related diseases, gastrointestinal diseases, and

431   cancers. It is unclear why pastoralists would have the lowest risk in these specific

432   disease categories. We caution that this pattern may be the result of technical issues,

433   as pastoralists have the smallest sample size (only 19 individuals) and geographic

434   range (between 40-90°E longitude and 45-55°N latitude, Figure 1B). Because

435   populations that have different subsistence types also differ in other ways, the lower

436   GRS of pastoral populations may be due to other factors, including demographic

437   history.

438   Comparisons amongst ancient individuals suggest that the transition to

439   agriculture brought about changes not only to diet, but also genetic risk for certain

440   diseases. Based on genomic data, we inferred that ancient agriculturalists had

441   increased risk for dental caries and periodontal diseases. However, slight caution is

442   advised about over interpreting this pattern as dental caries and periodontal diseases

443   had the smallest number of risk loci (k = 40). Previous comparisons of ancient skeletal

444   remains showed that hunter-gatherers had fewer caries than early agriculturalists

445   (Tillier, et al. 1995; Kerr 1998; Trinkaus, et al. 2000; Lebel and Trinkaus 2002). The

446   greater prevalence of dental caries in early agriculturalists may be partially due to

20

447   differences in oral microbiota diversity, as ancient hunter-gatherers were less likely to

448   have periodontal disease-associated taxa in calcified dental plaques (Adler, et al. 2013).

449   We note that genomic health does not necessarily equate to phenotypic health.

450   Genetic risk scores are not deterministic, instead they merely indicate whether an

451   individual has a predisposition to a particular disease. In addition, alleles that contribute

452   to disease in modern environments may not have had the same effects in past

453   environments. Because of the large genetic distances between modern humans and

454   archaic hominins, we caution against over-interpreting genomic estimates of

455   Neanderthal and Denisovan health.

456   Genomic studies, such as this one, provide an opportunity for incomplete or

457   poorly preserved ancient samples to contribute valuable information about the health

458   and disease status of our ancestors. As more ancient hominin genomes are sequenced

459   and new disease-associated loci are identified, there will be unprecedented

460   opportunities to probe changes in human health over time.

LITERATURE CITED

Abi-Rached L, Jobin MJ, Kulkarni S, McWhinnie A, Dalva K, Gragert L, Babrzadeh F, Gharizadeh B, Luo M, Plummer FA, et al. 2011. The Shaping of Modern Human Immune Systems by Multiregional Admixture with Archaic Humans. Science 334:89-94.

Adler CJ, Dobney K, Weyrich LS, Kaidonis J, Walker AW, Haak W, Bradshaw CJA, Townsend G, Soltysiak A, Alt KW, et al. 2013. Sequencing ancient calcified dental plaque shows changes in oral microbiota with dietary shifts of the Neolithic and Industrial revolutions. Nature Genetics 45:450-455.

Andrushko VA, Verano JW. 2008. Prehistoric trepanation in the Cuzco region of Peru: A view into an ancient Andean practice. American Journal of Physical Anthropology 137:4-13.

Binder M, Roberts C, Spencer N, Antoine D, Cartwright C. 2014. On the Antiquity of Cancer: Evidence for Metastatic Carcinoma in a Young Man from Ancient Nubia (c. 1200BC). Plos One 9.

Burdett T, Hall P, Hasting E, Hindorff L, Junkins H, Klemm A, MacArthur J, Manolio T, Morales J, Parkinson H. 2016. The NHGRI-EBI Catalog of published genome-wide association studies. Available at: www. ebiacuk/gwas.

Chang W, Cheng J, Allaire J, Xie Y, McPherson J. 2017. Shiny: web application framework for R. R package version 1.03.

Chatterjee N, Shi J, Garcia-Closas M. 2016. Developing and evaluating polygenic risk prediction models for stratified disease prevention. Nat Rev Genet 17:392-406.

483   Cordain L, Eaton SB, Sebastian A, Mann N, Lindeberg S, Watkins BA, O'Keefe JH,

484   Brand-Miller J. 2005. Origins and evolution of the Western diet: health

485   implications for the 21st century. American Journal of Clinical Nutrition 81:341-

486   354.

487   Corona E, Chen R, Sikora M, Morgan AA, Patel CJ, Ramesh A, Bustamante CD, Butte

488   AJ. 2013. Analysis of the genetic basis of disease in the context of worldwide

489   human relationships and migration. PLoS Genet 9:e1003447.

490   Dannemann M, Andres AM, Kelso J. 2016. Introgression of Neandertal- and Denisovan-

491   like Haplotypes Contributes to Adaptive Variation in Human Toll-like Receptors

492   (vol 98, pg 22, 2016). American Journal of Human Genetics 98:399-399.

493   Deschamps M, Laval G, Fagny M, Itan Y, Abel L, Casanova JL, Patin E, Quintana-Murci

494   L. 2016. Genomic Signatures of Selective Pressures and Introgression from

495   Archaic Hominins at Human Innate Immunity Genes. American Journal of Human

496   Genetics 98:5-21.

497   Entezami P, Fox DA, Clapham PJ, Chung KC. 2011. Historical perspective on the

498   etiology of rheumatoid arthritis. Hand Clin 27:1-10.

499   Field Y, Boyle EA, Telis N, Gao ZY, Gaulton KJ, Golan D, Yengo L, Rocheleau G,

500   Froguel P, McCarthy MI, et al. 2016. Detection of human adaptation during the

501   past 2000 years. Science 354:760-764.

502   Hawks J, Wang ET, Cochran GM, Harpending HC, Moyzis RK. 2007. Recent

503   acceleration of human adaptive evolution. Proc Natl Acad Sci U S A 104:20753-

504   20758.

505   Hofreiter M, Paijmans JL, Goodchild H, Speller CF, Barlow A, Fortes GG, Thomas JA,

506   Ludwig A, Collins MJ. 2015. The future of ancient DNA: Technical advances and

507   conceptual shifts. Bioessays 37:284-293.

508   Keller A, Graefen A, Ball M, Matzas M, Boisguerin V, Maixner F, Leidinger P, Backes C,

509   Khairat R, Forster M, et al. 2012. New insights into the Tyrolean Iceman's origin

510   and phenotype as inferred by whole-genome sequencing. Nat Commun 3:698.

511   Kerr NW. 1998. Prevalence and natural history of periodontal disease in prehistoric

512   Scots (pre-900 AD). J Periodontal Res 33:131-137.

513   Lachance J. 2010. Disease-associated alleles in genome-wide association studies are

514   enriched for derived low frequency alleles relative to HapMap and neutral

515   expectations. BMC Med Genomics 3:57.

516   Lachance J, Tishkoff SA. 2013. SNP ascertainment bias in population genetic analyses:

517   why it is important, and how to correct it. Bioessays 35:780-786.

518   Lazaridis I, Nadel D, Rollefson G, Merrett DC, Rohland N, Mallick S, Fernandes D,

519   Novak M, Gamarra B, Sirak K, et al. 2016. Genomic insights into the origin of

520   farming in the ancient Near East. Nature 536:419-424.

521   Lebel S, Trinkaus E. 2002. A carious Neandertal molar from the Bau-de-l'Aubesier,

522   Vaucluse, France. Journal of Archaeological Science 29:555-557.

523   Li H. 2011. A statistical framework for SNP calling, mutation discovery, association

524   mapping and population genetical parameter estimation from sequencing data.

525   Bioinformatics 27:2987-2993.

526 Li H, Handsaker B, Wysoker A, Fennell T, Ruan J, Homer N, Marth G, Abecasis G,

527   Durbin R, Genome Project Data Processing S. 2009. The Sequence

528   Alignment/Map format and SAMtools. Bioinformatics 25:2078-2079.

529 Li Y, Willer C, Sanna S, Abecasis G. 2009. Genotype imputation. Annu Rev Genomics

530   Hum Genet 10:387-406.

531 Lynch M. 2016. Mutation and Human Exceptionalism: Our Future Genetic Load.

532   Genetics 202:869-875.

533 MacArthur J, Bowler E, Cerezo M, Gil L, Hall P, Hastings E, Junkins H, McMahon A,

534   Milano A, Morales J. 2017. The new NHGRI-EBI Catalog of published genome-

535   wide association studies (GWAS Catalog). Nucleic acids research 45:D896-

536   D901.

537 Mathieson I, Lazaridis I, Rohland N, Mallick S, Patterson N, Roodenberg SA, Harney E,

538   Stewardson K, Fernandes D, Novak M, et al. 2015. Genome-wide patterns of

539   selection in 230 ancient Eurasians. Nature 528:499-503.

540 Murphy WA, Jr., Nedden Dz D, Gostner P, Knapp R, Recheis W, Seidler H. 2003. The

541   iceman: discovery and imaging. Radiology 226:614-629.

542 Odes EJ, Randolph-Quinney PS, Steyn M, Throckmorton Z, Smilg JS, Zipfel B,

543   Augustine TN, de Beer F, Hoffman JW, Franklin RD, et al. 2016. Earliest hominin

544   cancer: 1.7-million-year-old osteosarcoma from Swartkrans Cave, South Africa.

545   South African Journal of Science 112:100-104.

546 Orlando L, Gilbert MT, Willerslev E. 2015. Reconstructing ancient genomes and

547   epigenomes. Nat Rev Genet 16:395-408.

548   Roth FP, Wakeley J. 2016. Taking Exception to Human Eugenics. Genetics 204:821-

549   823.

550   Sainz S, Soriano G, Guarner C, Coll P, Vilardell F. 1989. More on ascitic fluid culture

551   technique. Hepatology 9:662-663.

552   Simonti CN, Vernot B, Bastarache L, Bottinger E, Carrell DS, Chisholm RL, Crosslin

553   DR, Hebbring SJ, Jarvik GP, Kullo IJ, et al. 2016. The phenotypic legacy of

554   admixture between modern humans and Neandertals. Science 351:737-741.

555   The 1000 Genomes Project Consortium. 2015. A global reference for human genetic

556   variation. Nature 526:68-74.

557   Tillier AM, Arensburg B, Rak Y, Vandermeersch B. 1995. Middle Paleolithic Dental-

558   Caries - New Evidence from Kebara (Mount Carmel, Israel). Journal of Human

559   Evolution 29:189-192.

560   Trinkaus E, Smith RJ, Lebel S. 2000. Dental caries in the Aubesier 5 Neandertal

561   primary molar. Journal of Archaeological Science 27:1017-1021.

562

TABLES

564

565 **Table 1**. Results of statistical tests between ancient hominin genetic risk scores compared to modern humans (Wilcoxon

566 signed rank test) and amongst ancient samples by sample age range (years BP; Jonckheere-Terpstra test), mode of

567 subsistence (Krustal-Wallis test), and geographic location (latitude and longitude; Pearson's correlation tests). Boldface

568 indicates that the p-value is less than 0.05.

569

Disease Type (number of loci)	Relative to present-day		Sample age range		Subsistence		Latitude			Longitude		
	V	p-value	JT	p-value	χ^2	p-value	r	t	p-value	r	t	p-value
All Diseases (3180)	3266	**2.6×10^{-5}**	5275	**1.0×10^{-3}**	12.34	**2.0×10^{-3}**	-0.23	-2.86	**5.0×10^{-3}**	-0.13	-1.61	0.11
Allergy/Autoimmune (770)	5028	0.51	4775.5	**0.035**	7.41	**0.02**	-0.06	-0.69	0.49	-0.09	-1.09	0.28
Cancers (644)	4083	**0.03**	5049	2.0×10^{-3}	9.73	**0.01**	-0.29	-3.71	**3.0×10^{-4}**	-0.08	-0.94	0.35
Cardiovascular (232)	7659.5	**1.8×10^{-5}**	4523.5	0.18	3.26	0.20	-0.06	-0.70	0.49	-0.20	-2.44	**0.02**
Dental/Periodontal (40)	6203	0.10	4310.5	0.38	14.15	**8.5×10^{-4}**	-0.20	-2.48	**0.01**	-0.13	-1.57	0.12
Gastrointestinal/Liver (488)	4553	0.09	4770	**0.033**	17.82	**1.4×10^{-4}**	-0.15	-1.83	0.07	-0.12	-1.49	0.14
Metabolism/Weight (309)	5052.5	0.54	4674	0.054	2.29	0.32	-0.13	-1.58	0.12	0.03	0.42	0.68
Miscellaneous (532)	3228	**1.9×10^{-5}**	4451	0.24	3.63	0.16	-0.06	-0.74	0.46	-3.2×10^{-3}	-0.04	0.97
Morphological/Muscular (239)	5898	0.38	4291.5	0.42	3.62	0.16	0.14	1.70	0.09	-0.14	-1.66	0.10
Neurological/Psychological (459)	2823	**1.8×10^{-6}**	4451.5	0.25	2.83	0.24	0.01	0.12	0.90	2.8×10^{-3}	0.03	0.97

570

571 **Table 2**. Statistical results of ancient genetic risk score comparisons between

572 subsistence types (AG – Agriculturalist; PA – Pastoralist; HG – Hunter-Gatherer) from

573 Dunn tests with Benjamini-Hochberg correction, which were performed on disease

574 categories with significant differences between subsistence groups (see Table 1).

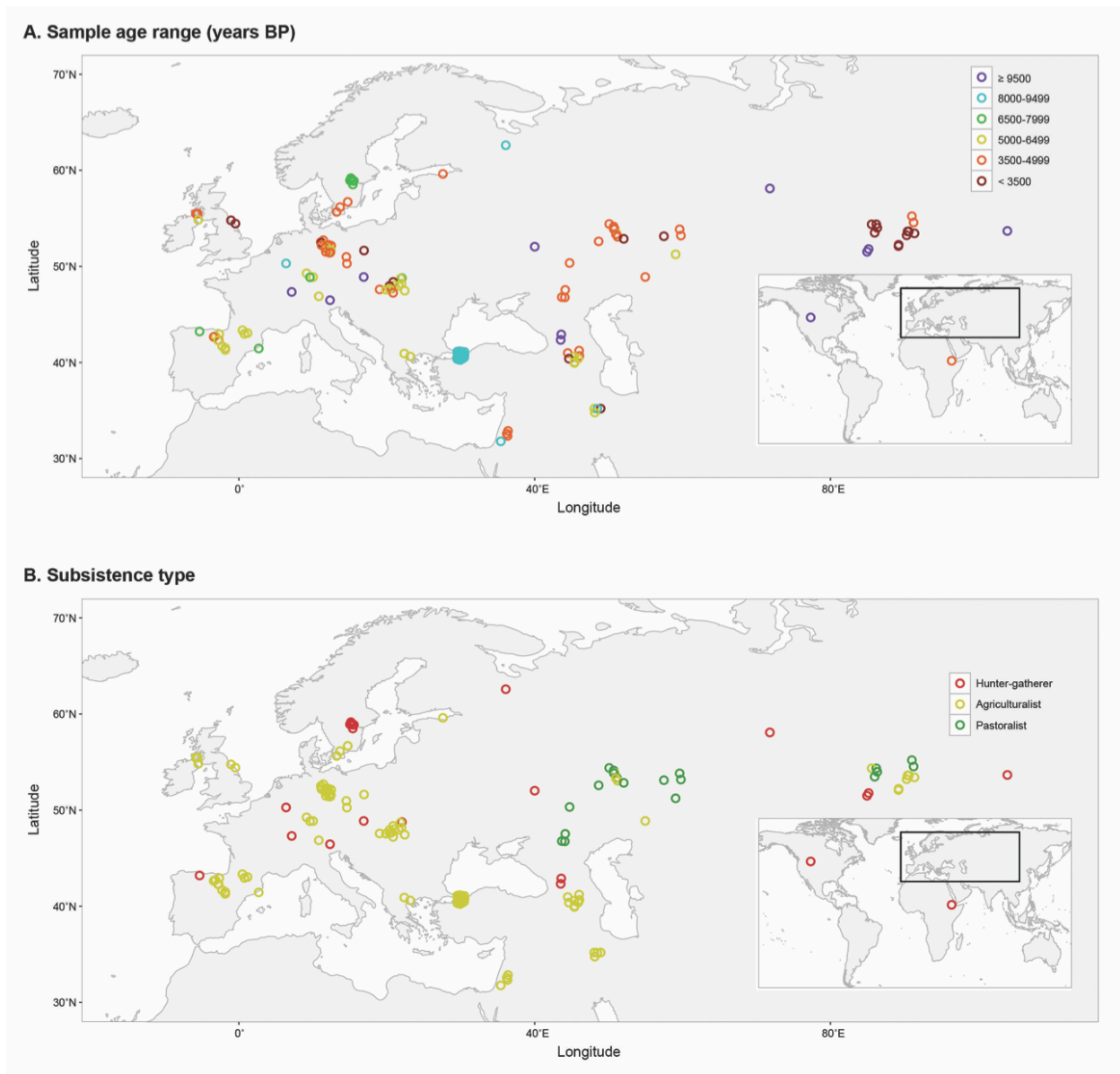575 Boldface indicates that the p-value is less than 0.05.

576

	AG vs HG		AG vs PA		HG vs PA	
	z	p-value	z	p-value	z	p-value
All Diseases	-1.35	0.09	2.98	**2.1×10^{-3}**	3.38	**1.1×10^{-3}**
Allergy/Autoimmune	-1.40	0.08	2.08	**0.03**	2.70	**0.01**
Cancers	0.90	0.18	3.09	**3.0×10^{-3}**	1.78	0.06
Dental/Periodontal	3.04	**3.5×10^{-3}**	2.67	**5.7×10^{-3}**	-0.15	0.44
Gastrointestinal/Liver	0.98	0.16	4.21	**$<1.0 \times 10^{-3}$**	2.61	**6.8×10^{-3}**

577

28

578   **FIGURES**

579   **Figure 1**

Figure 1: Location, age, and subsistence type of ancient hominins. Geographic

distribution of 147 ancient individuals by (A) sample age range in years BP and (B)

subsistence type. Over 50% of all disease-associated variants were successfully called

for each individual, and geographical locations were jittered to clarify densely sampled

locations.

586 **Figure 2**
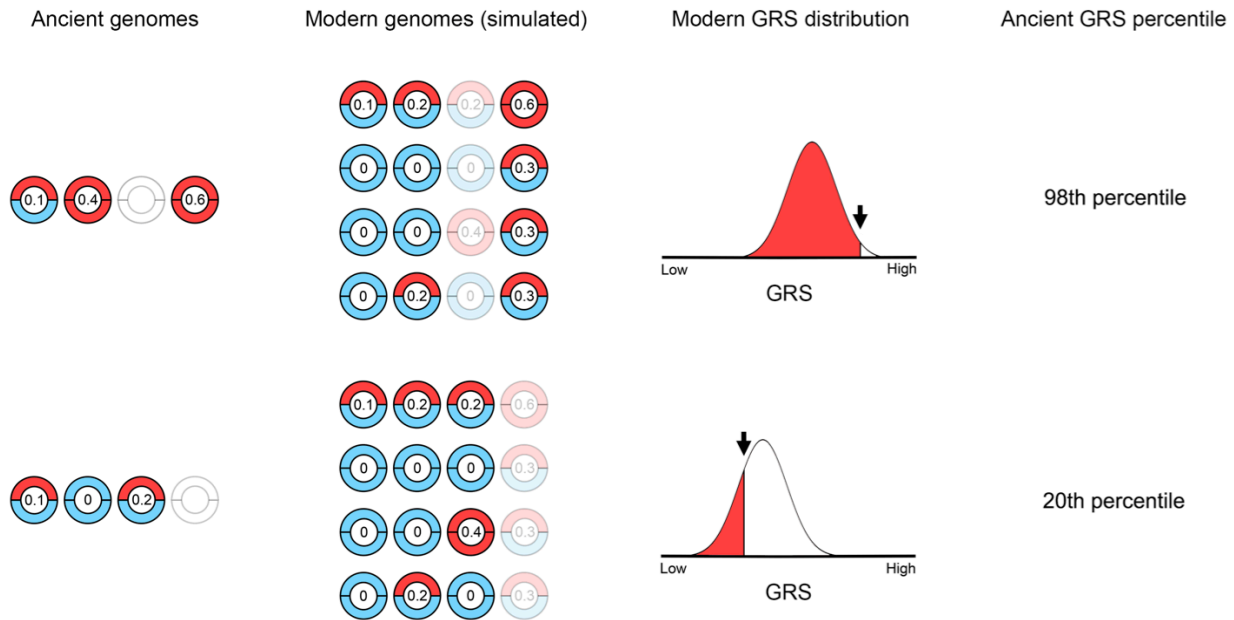
587

588

589 **Figure 2**: Schematic of how standardized GRS percentiles were estimated for each

590 ancient sample. PokéPlots are shown for each disease locus. Risk alleles are indicated

591 by a red hemisphere, protective alleles are indicated by a blue hemisphere, and

592 numbers denote beta coefficients. Disease loci without genotypic information in the

593 focal ancient individual are masked when estimating GRS for simulated modern

594 humans. Ancient GRS are compared to the distribution of the simulated modern GRS to

595 determine the ancient standardized GRS percentile. The simulated modern GRS

596 distribution differs for each ancient hominin based on which disease loci have known

597 genotypic information.

598 **Figure 3**
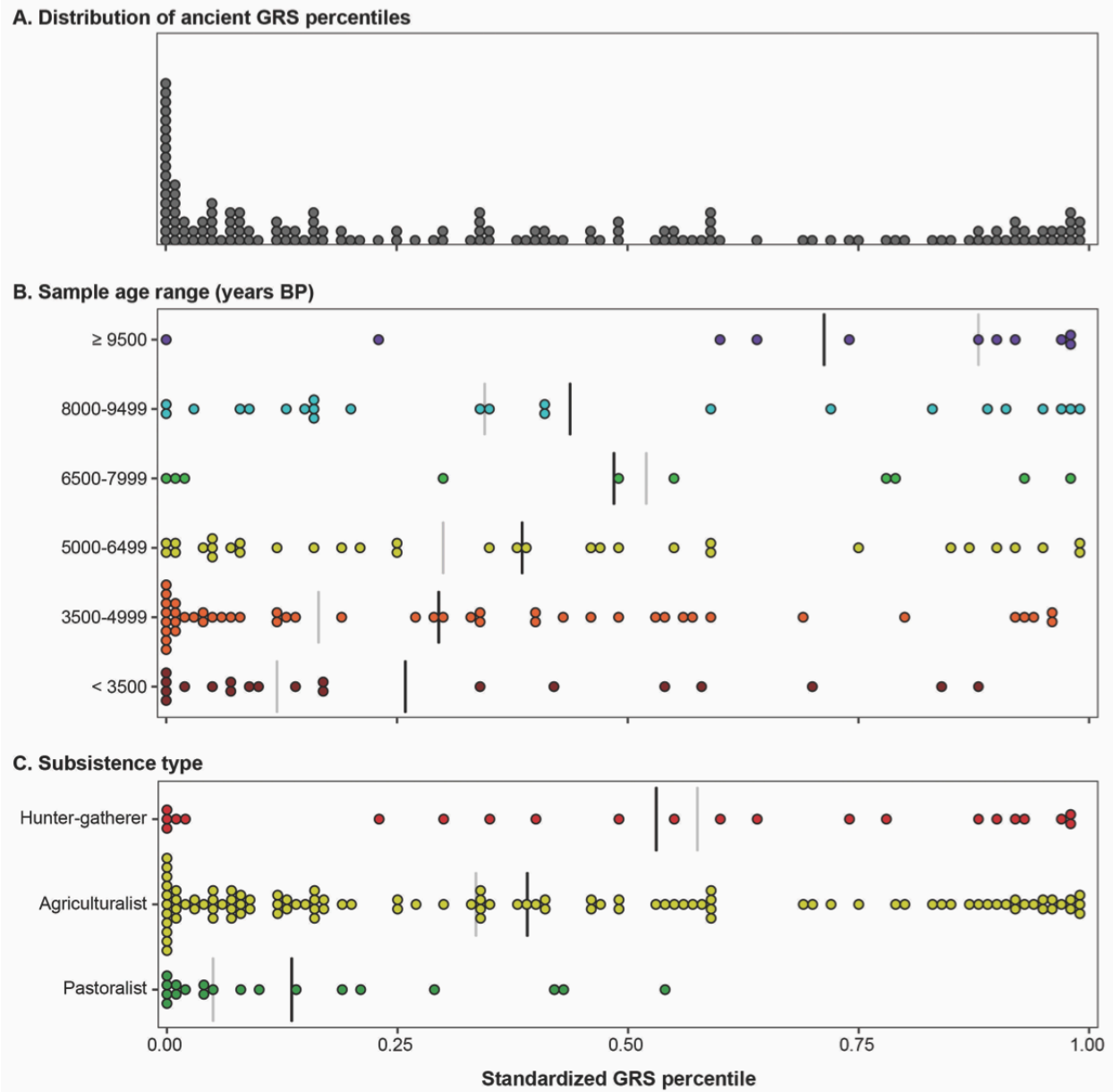
Figure 3: Ancient genetic risk scores span the full range of modern humans. (A) The distribution of ancient standardized GRS percentiles, which includes an excess of healthy individuals below the 5th percentile. Ancient standardized GRS percentiles separated by (B) age range and (C) subsistence type. Group means indicated by black line and group medians denoted by grey line.

31

605   **Figure 4**
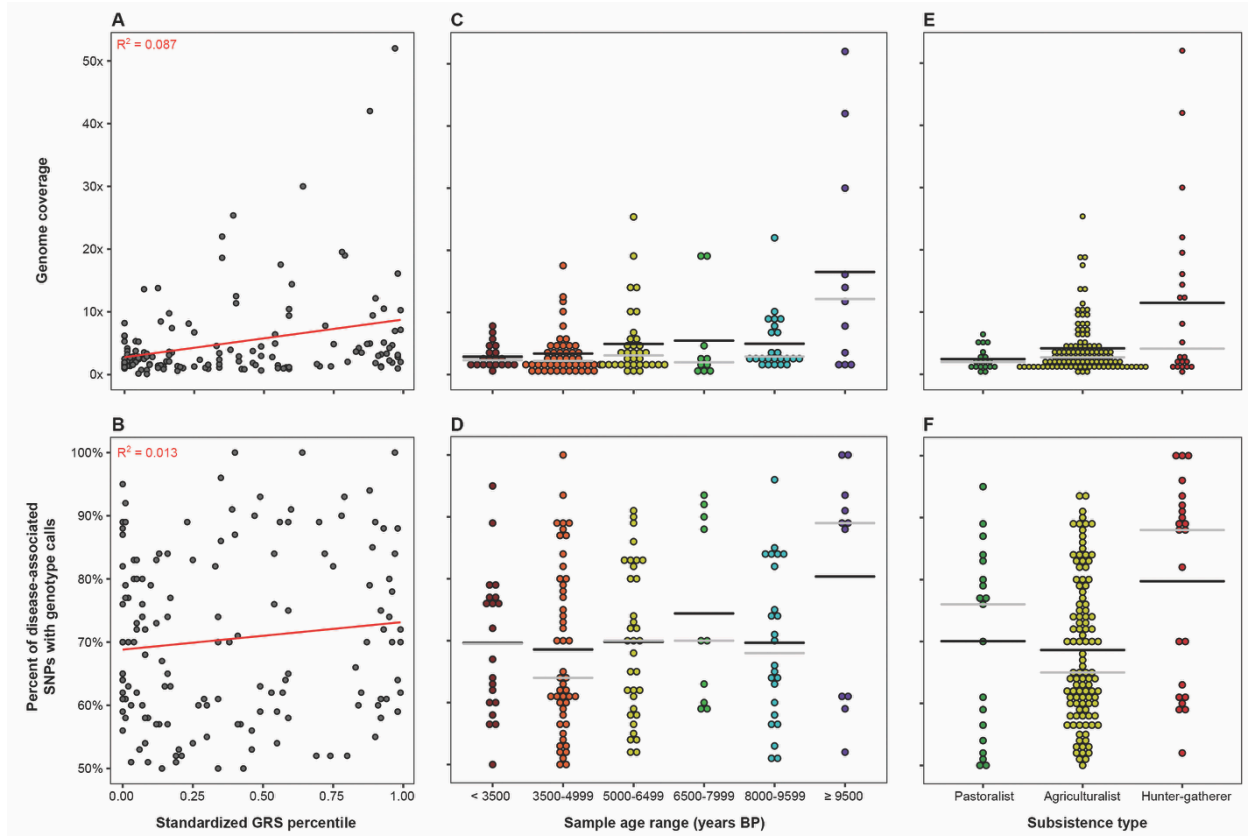
606

607

608   **Figure 4**: Sequence coverage and sample quality have minimal effect on genetic risk
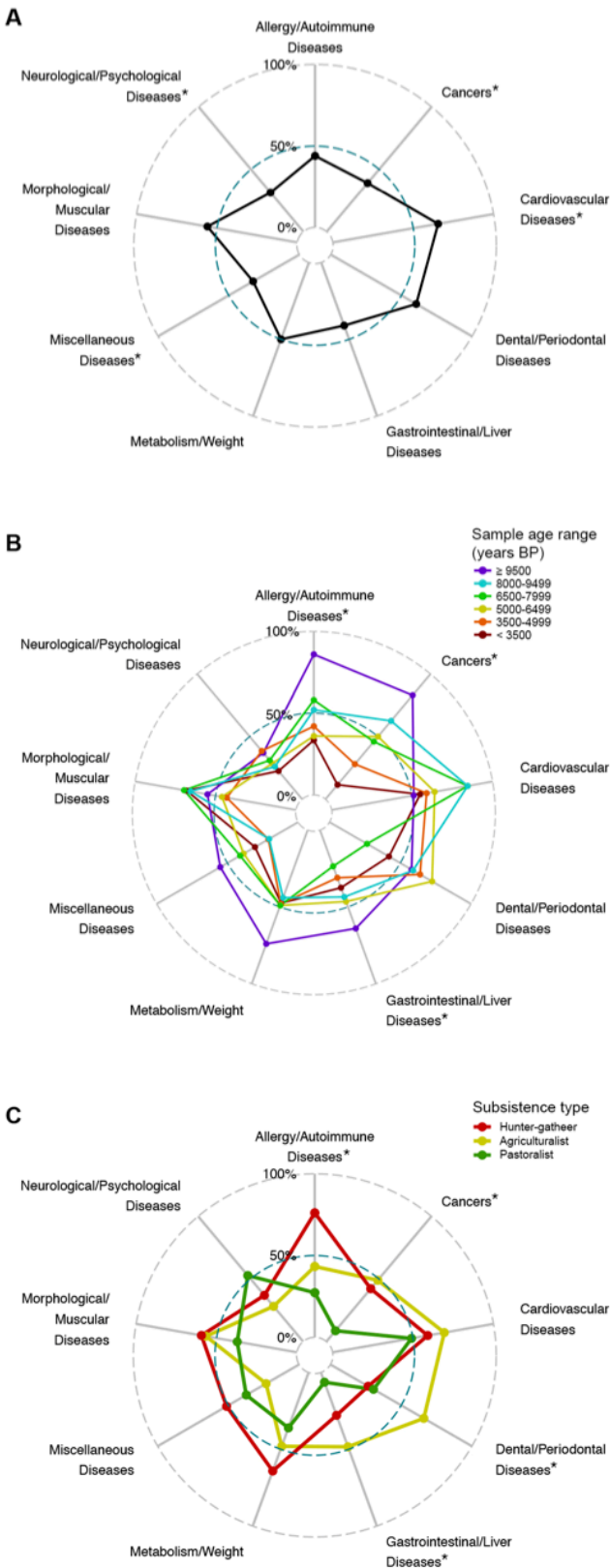
609   scores. Genome coverage (top) and proportion of disease-associated loci called

610   (bottom) by genetic risk percentile (left), age range (center), and subsistence type

611   (right). Group means and medians indicated by black and grey lines, respectively.

612

613 **Figure 5**

614

615   **Figure 5**: Risk radars of genomic health for ancient samples. The length of each spoke

616   corresponds to a standardized GRS percentile. Healthy individuals have smaller shapes

617   in risk radar plots. (A) Standardized GRS percentile by disease category for all ancient

618   hominins summarized as median risk score. The median of genetic disease risk in

619   modern humans is the 50th percentile. Temporal (B) and subsistence (C) trends of

620   median ancient genetic risk by disease category. Disease categories with significant

621   differences (p-value < 0.05) from Table 1 are denoted by *.

34